

See discussions, stats, and author profiles for this publication at: <https://www.researchgate.net/publication/231443632>

Repulsive Coulomb Barriers in Compact Stable and Metastable Multiply Charged Anions

ARTICLE *in* JOURNAL OF THE AMERICAN CHEMICAL SOCIETY · NOVEMBER 2000

Impact Factor: 12.11 · DOI: 10.1021/ja001936a

CITATIONS

60

READS

26

3 AUTHORS, INCLUDING:



Piotr Skurski

University of Gdansk

141 PUBLICATIONS 3,391 CITATIONS

SEE PROFILE

Repulsive Coulomb Barriers in Compact Stable and Metastable Multiply Charged Anions

Jack Simons,* Piotr Skurski,[†] and Robyn Barrios

Contribution from the Chemistry Department, University of Utah, Salt Lake City, Utah 84112

Received June 1, 2000. Revised Manuscript Received September 8, 2000

Abstract: We demonstrate that a simple Coulomb-energy model can be used to predict the vertical electron detachment energy of an anion of charge $(-n)$ given the detachment energy of the corresponding anion having one less charge $(-n + 1)$. This model was applied earlier by other workers to dianions in which the two charged sites are quite distant. In this paper we show that it can also be applied to more spatially compact species as long as the two orbitals from which the electrons are removed are sufficiently noninteracting. We first demonstrate how to use this model by applying it to a series of electronically stable dianions (MgF_4^{2-} , BeF_4^{2-} , TeF_8^{2-} , SeF_8^{2-} , and TeCl_8^{2-}) for which the (-2) to (-1) and (-1) to (neutral) electron detachment energies have been evaluated using conventional ab initio methods. These test calculations allow us to assess the predictive accuracy of the Coulomb model. We then extend the model's use to predict the energies of dianions and trianions that are not electronically stable (SO_4^{2-} , CO_3^{2-} , PO_4^{3-} , and PO_4^{2-}) and for which application of conventional quantum chemistry methods will not yield reliable predictions. That is, we predict at what energies metastable resonance states of these species will occur. Finally, we use the Coulomb nature of the long-range part of the electron–anion potential to estimate the lifetimes of these resonance states with respect to electron loss.

I. Introduction

In recent years, significant advances in the experimental¹ and theoretical² study of multiply charged anions have been realized. On the experimental front, beautiful laser detachment and photoelectron experiments from the Wang group¹ have produced a plethora of new data that have prompted theoreticians to assist in their interpretation. One of the most important concepts¹ to have arisen in understanding such spectra of multiply charged anions is that of the repulsive Coulomb barrier (RCB). To illustrate this concept and its utility, we display in Figure 1 the electron binding energies (EBE) determined from peaks³ in the detachment spectra of a series of dicarboxylates $^-\text{O}_2\text{C}-(\text{CH}_2)_n-\text{CO}_2^-$. The electron binding energy data clearly fit a linear

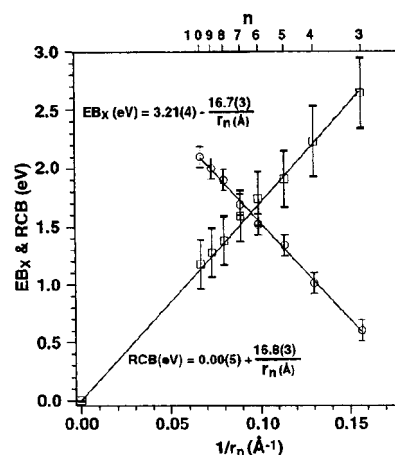


Figure 1. Plots of the electron binding energies and repulsive Coulomb barriers pertinent to $^-\text{O}_2\text{C}-(\text{CH}_2)_n-\text{CO}_2^-$ dianions. Reprinted with permission from ref 1f. Copyright 2000, American Chemical Society.

functional form whose large n intercept is ca. 3.2 eV, which represents the electron binding energy of a singly charged carboxylate anion such as $\text{H}_3\text{C}-\text{CO}_2^-$.⁴ To remove an electron from one of the two carboxylate groups in a chain of finite length does not require as much energy as for the singly charged carboxylate because of the Coulomb repulsion energy generated by the other carboxylate group's negative charge. This Coulomb repulsion can be thought of as raising the energy level of the bound electron by an amount e^2/R_n that depends on the distance R_n between the electron being detached and the other negatively charged site. Clearly, this distance depends linearly on the number of methylene groups for the example at hand,⁵ and thus, the EBE varies linearly when plotted vs $1/R_n$.

[†] Permanent address: University of Gdańsk, Department of Chemistry, 80-952 Gdańsk, Poland.

(1) (a) Compton, R. N. *Negative Ion States*. In *Photophysics and Photochemistry in the Vacuum Ultraviolet*; McGlynn, S. P., et al., Eds.; Reidel: The Netherlands, 1985. (b) Schauer, S. N.; Williams, P.; Compton, R. N. *Phys. Rev. Lett.* **1990**, *65*, 625. (c) Jin, C.; Hettich, R. L.; Compton, R. N.; Tuinman, A. A.; Derecskei-Kovacs, A.; Marynick, D. S.; Dunlap, B. I. *Phys. Rev. Lett.* **1994**, *73*, 2821. (d) Compton, R. N.; Tuinman, A. A.; Klots, C. E.; Pederson, M. R.; Patton, D. C. *Phys. Rev. Lett.* **1997**, *78*, 4367. (e) Wang, L. S. *Comments At. Mol. Phys.* **2000**, in press. (f) Wang, L. S.; Wang, X. B. *J. Phys. Chem. A* **2000**, *104*, 1978. (g) Wang, X. B.; Ding, C. F.; Wang, L. S. *Phys. Rev. Lett.* **1998**, *81*, 3351. (h) Wang, L. S.; Ding, C. F.; Wang, X. B.; Nicholas, J. B. *Phys. Rev. Lett.* **1998**, *81*, 2667. (i) Ding, C. F.; Wang, X. B.; Wang, L. S. *J. Phys. Chem. A* **1998**, *102*, 8633. (j) Wang, X. B.; Ding, C. F.; Wang, L. S. *Chem. Phys. Lett.* **1999**, *307*, 391. (k) Ding, C. F.; Wang, X. B.; Wang, L. S. *J. Chem. Phys.* **1999**, *110*, 3635. (l) Wang, X. B.; Ding, C. F.; Nicholas, J. B.; Dixon, D. A.; Wang, L. S. *J. Phys. Chem. A* **1999**, *103*, 3423. (m) Skurski, P.; Simons, J.; Wang, X.-B.; Wang, L.-S. *J. Am. Chem. Soc.* **2000**, *122*, 4499. (n) Wang, X. B.; Wang, L. S. *J. Chem. Phys.* **1999**, *111*, 4497. (o) Wang, X. B.; Wang, L. S. *Nature* **1999**, *400*, 245. (p) Wang, X. B.; Ferris, K.; Wang, L. S. *J. Phys. Chem. A* **2000**, *104*, 25. (q) Wang, X. B.; Wang, L. S. *Phys. Rev. Lett.* **1999**, *83*, 3402. (r) Wang, X. B.; Wang, L. S. *J. Am. Chem. Soc.* **2000**, *122*, in press. (s) Wang, X. B.; Wang, L. S. *J. Phys. Chem. A* **2000**, *104*, in press. (t) Middleton, R.; Klein, J. *Phys. Rev. A* **1999**, *60*, 3515. (u) Gnaser, H. *Phys. Rev. A* **1999**, *60*, R2645.

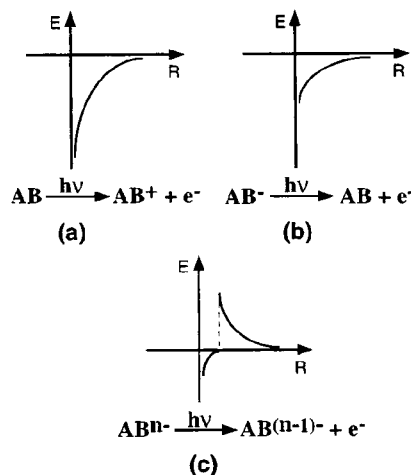


Figure 2. Qualitative descriptions of radial potentials appropriate to (a) an electron leaving a neutral molecule to form a cation, (b) an electron detached from a singly charged anion, and (c) an electron departing from an anion of charge $(-n)$. Reprinted with permission from ref 1f. Copyright 2000, American Chemical Society.

II. The Repulsive Coulomb Barrier

Let us explore further the nature and impact of this repulsive Coulomb potential that has both a destabilizing influence (as discussed above) and a stabilizing influence, as we now illustrate. In Figure 2 we provide qualitative illustrations of the radial potential experienced by an electron that is (a) detached from a neutral species, (b) detached from a singly charged anion, or (c) detached from an anion of charge $(-n)$ with $n > 1$. In the first case, the ejected electron experiences an *attractive* Coulomb potential as it leaves the region of the valence orbitals of the molecule because a cation is created when the electron departs. In case b, the ejected electron experiences attractive potentials of shorter range as it leaves the region of the valence orbitals. The nature of these attractive potentials depends on the electrostatic and induced moments of the neutral molecule that is left behind. However, an electron leaving a multiply

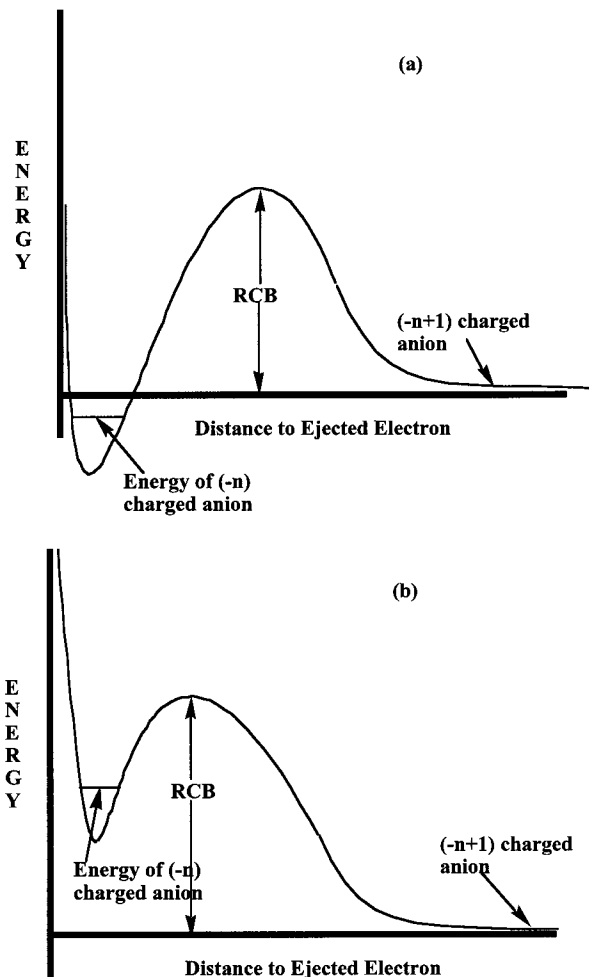


Figure 3. Effective radial potentials experienced by an electron in an anion of charge $(-n)$ when (a) the valence attractive potential is stronger than the repulsive Coulomb potential so a bound state exists and (b) when the valence attractive potential is weaker so a metastable state occurs.

charged anion experiences both attractive and repulsive potentials. At the longest range, the Coulomb repulsive potential caused by the $(-n + 1)$ charged anion that remains is dominant. However, at intermediate ranges, the Coulomb repulsion combines with the valence-range attractive potentials that act to bind the electron. It is the combination of valence-range attractive and long-range Coulomb repulsion that causes the changes in EDEs shown in Figure 1.

A. The RCB Can Destabilize Bound States. If the attractive valence potentials are stronger in the valence region than is the repulsive Coulomb potential, then a total potential such as illustrated in Figure 3a results. In such a case, the lowest bound state of the $(-n)$ charged anion lies below the lowest state of the $(-n + 1)$ charged anion, so the former is electronically stable. Moreover, the total potential will display a characteristic repulsive Coulomb barrier (RCB) in the region where the Coulomb potential is overtaken by the valence-range potential. The height of this RCB can be approximated by computing e^2/R , where R is the distance between the ejected electron's orbital and the other negatively charged site(s).

As Wang and co-workers have shown, attempts to detach electrons from a $(-n)$ charged species using photons whose energy lies significantly below the top of the RCB fail. Photons that excite the $(-n)$ charged anion near or above the RCB are necessary. The RCB thus also plays an important role in determining the shape of the photodetachment spectra by shifting

(2) (a) Scheller, M. K.; Compton, R. N.; Cederbaum, L. S. *Science* **1995**, 270, 1160. (b) Kalcher, J.; Sax, A. F. *Chem. Rev.* **1994**, 94, 2291. (c) Scheller, M. K.; Cederbaum, L. S. *J. Chem. Phys.* **1993**, 99, 441. (d) Scheller, M. K.; Cederbaum, L. S. *J. Chem. Phys.* **1994**, 100, 8934. (e) Sommerfeld, T.; Scheller, M. K.; Cederbaum, L. S. *J. Chem. Phys.* **1995**, 103, 1057. (f) Weikert, H. G.; Meyer, H. D.; Cederbaum, L. S. *J. Chem. Phys.* **1996**, 104, 7122. (g) Dreuw, A.; Sommerfeld, T.; Cederbaum, L. S. *J. Chem. Phys.* **1998**, 109, 2727. (h) Zakrzewski, V. G.; Ortiz, J. V. *J. Chem. Phys.* **1995**, 102, 294. (i) Enlow, M.; Ortiz, J. V.; Luthi, H. P. *Mol. Phys.* **1997**, 92, 441. (j) Dolgounitcheva, O.; Zakrzewski, V. G.; Ortiz, J. V. *J. Chem. Phys.* **1998**, 109, 87. (k) Boldyrev, A. I.; Simons, J. *J. Chem. Phys.* **1992**, 97, 2826. (l) Boldyrev, A. I.; Simons, J. *J. Chem. Phys.* **1993**, 98, 4745. (m) Boldyrev, A. I.; Simons, J. *J. Phys. Chem.* **1994**, 98, 2293. (n) Gutowski, M.; Boldyrev, A. I.; Ortiz, J. V.; Simons, J. *J. Am. Chem. Soc.* **1994**, 116, 9262. (o) Gutowski, M.; Boldyrev, A. I.; Simons, J.; Rak, J.; Blazewski, J. *J. Am. Chem. Soc.* **1996**, 118, 1173. (p) Boldyrev, A. I.; Gutowski, M.; Simons, J. *Acc. Chem. Res.* **1996**, 29, 497. (q) tefanovich, E. V.; Boldyrev, A. I.; Truong, T. N.; Simons, J. *J. Phys. Chem. B* **1998**, 102, 4205. (r) Adamowicz, L. *J. Chem. Phys.* **1991**, 95, 8669. (s) Watts, J. D.; Bartlett, R. J. *J. Chem. Phys.* **1992**, 97, 3445. (t) Zakrzewski, V. G.; Ortiz, J. V. *J. Chem. Phys.* **1995**, 102, 294. (u) Enlow, M.; Ortiz, J. V.; Luthi, H. P. *Mol. Phys.* **1997**, 92, 441. (v) Dolgounitcheva, O.; Zakrzewski, V. G.; Ortiz, J. V. *J. Chem. Phys.* **1998**, 109, 87.

(3) Vertical binding energies are usually determined from the maxima in the lowest detachment channel.

(4) See, for example: Skurski, P.; Simons, J.; Wang, X.-B.; Wang, L.-S. *J. Am. Chem. Soc.* **2000**, 122, 4499.

(5) This assumes that the dianion adopts as linear a geometry as possible. Although it is not true in solution that such flexible hydrocarbon chains adopt such conformations, it is likely in the gas phase that the mutual Coulomb repulsion of the two carboxylate groups causes the chain to be so aligned. Moreover, the fact that the EDE data can be fit to a model that assumes such a linear arrangement provides support for this assumption.

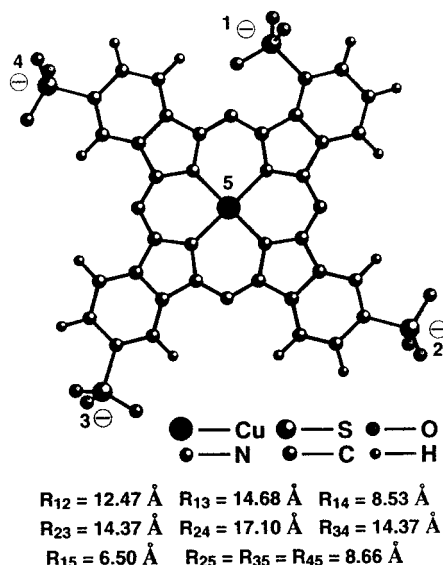


Figure 4. Structure of the $\text{CuPc}(\text{SO}_3^-)_4$ anion showing the location of the four $-\text{SO}_3^-$ groups relative to the central Cu atom. Reprinted with permission from ref 1f. Copyright 2000, American Chemical Society.

the apparent threshold to energies not related to the actual adiabatic detachment energy but to the height of the RCB. For this reason, it has proven necessary to perform photoelectron experiments, in which the kinetic energies of the ejected electrons are measured with photons having energy in excess of the RCB, to determine EDEs in such multiply charged anions.

B. The RCB Can Give Rise to Metastable States. In contrast to the case illustrated in Figure 3a, if the Coulomb repulsion potential is strong enough to outweigh the attractive potentials in the valence region, a situation such as shown in Figure 3b can arise in which a metastable⁶ anion of charge $(-n)$ results. In such a case, the anion of charge $(-n)$ is electronically unstable with respect to the $(-n + 1)$ charged anion, but the RCB stabilizes the $(-n)$ anion by requiring the departing electron to tunnel through this barrier to escape. Indeed, in their study of the copper phthalocyanine, 3,4',4'', 4'''-tetrasulfonate $[\text{CuPc}(\text{SO}_3)_4]^{4-}$ system shown in Figure 4, Wang and co-workers⁷ monitored the lowest electron detachment threshold as the number of $-\text{SO}_3^-$ groups was varied from zero to four. With no $-\text{SO}_3^-$ groups attached, detaching an electron⁸ requires 6.7 eV as Figure 5a illustrates. Appending three $-\text{SO}_3^-$ groups (and one neutral $-\text{SO}_3\text{H}$ group) to the Pc ring system shifts the lowest electron binding energy from 6.7 to 1.2 eV as shown in Figure 5b. Finally, addition of a fourth $-\text{SO}_3^-$ group further shifts the electron binding energy by another 2.1 eV as shown in Figure 5c, indeed creating a situation in which the (-4) charged system is unstable by ca. 0.9 eV relative to the (-3) charged anion plus a free electron. In this case, photoelectron experiments found that the ejected electrons possessed higher kinetic energy than did the photon used to effect the electron

(6) In such a case, we speak of the $(-n)$ charged anion as being electronically metastable. Of course, these same Coulomb repulsions, if strong enough, can cause the $(-n)$ charged anion to break one or more chemical bonds and fragment into less-charged anions. In the present work, most of our attention is addressed to the issue of electronic stability or metastability. A good overview of the variety of metastable states that occur in chemical systems is given in: Simons, J. *Roles Played by Metastable States in Chemistry*. In *Resonances in Electron-Molecule Scattering, van der Waals Complexes, and Reactive Chemical Dynamics*; ACS Symp. Ser. No. 263; American Chemical Society: Washington, DC, 1984; pp 3–16.

(7) Wang, X.-B.; Wang, L.-S. *Nature* **1999**, *400*, 245.

(8) For this molecule, the electron is removed from a Cu d_{π} orbital localized in the center of the Cu–Pc π -orbital framework.

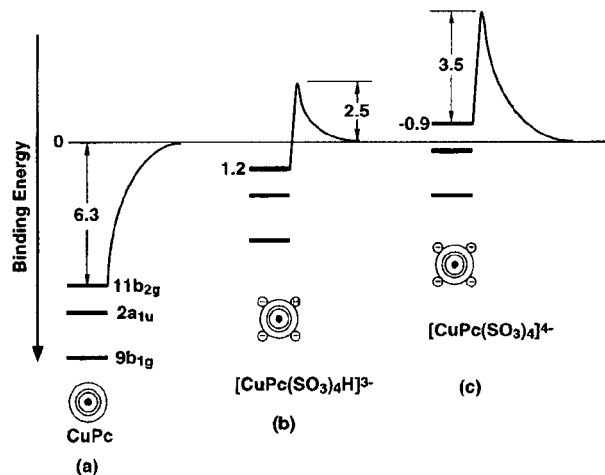


Figure 5. Radial potentials appropriate to (a) neutral CuPc, (b) $\text{CuPc}(\text{SO}_3^-)_3(\text{SO}_3\text{H})$, and (c) $\text{CuPc}(\text{SO}_3^-)_4$. Reprinted with permission from ref 1f. Copyright 2000, American Chemical Society.

detachment thus validating the claim that the (-4) charged species has a negative electron binding energy.

III. RCBs in More Compact Multiply Charged Anions

The validity and utility of the Coulomb repulsion energy model has been clearly demonstrated in a large number of cases by the Wang group and others.^{1–9} However, in the species that have been considered to date, it has been relatively clear how to compute the internal Coulomb energy because the (two or more) negatively charged sites have been reasonably well localized and have been rather distant one from the other(s). For example, in the $^-\text{O}_2\text{C}-(\text{CH}_2)_n-\text{CO}_2^-$ systems, the distance R_n between the two anion sites is primarily determined by the length of the methylene chain and the bond lengths in the $-\text{CO}_2$ units. The primary uncertainty relates to where near the terminal O atoms one defines the negative sites to reside (i.e., the uncertainty relates to the finite size of the orbital in which the “extra” electrons reside). In the $[\text{CuPc}(\text{SO}_3)_4]^{4-}$ system, the orbital from which an electron is detached is a Cu d orbital that is rather distant from the negatively charged $-\text{SO}_3^-$ groups. Hence, small uncertainties in defining where, within the $-\text{SO}_3^-$ groups, the negative charges reside produce very small uncertainties in the internal Coulomb energies (i.e., in the computed e^2/R values).

Another simplifying feature of more extended systems such as $^-\text{O}_2\text{C}-(\text{CH}_2)_n-\text{CO}_2^-$ relates to the nearly perfect degeneracy of the two orbitals containing the two excess electrons. Even if a symmetry element were present to cause the left $^-\text{O}_2\text{C}-$ and right $-\text{CO}_2^-$ orbitals to combine to form gerade (g) and ungerade (u) molecular orbitals, the energy splitting between the g and u orbitals would be very small. As a result, one can ascribe the computed electron detachment energy to the removal of an electron from the left or right carboxylate group. Formally, this can be shown by combining the two isoenergetic determinants ϕ_g and ϕ_u (one with the g orbital half filled, the second with the u orbital half filled) to form two new functions $2^{-1/2}(\phi_g \pm \phi_u)$ having the same energy, one of which has the left carboxylate orbital half filled while the second has the right orbital half filled. Although this observation may be obvious in cases such as the carboxylates where the two anion sites are very distant and thus noninteracting, it is by no means clear

(9) (a) Weis, P.; Hampe, O.; Gilb, S.; Kappes, M. *Chem. Phys. Lett.* **2000** *321*, 426. (b) Dreuw, A.; Cederbaum, L. S. *J. Chem. Phys.* **2000** *112*, 7400.

whether analogous simplifications occur in more spatially compact dianions. It is to be expected that these simplifications, which allow us to interpret electron detachment as occurring from localized site-centered orbitals rather than delocalized molecular orbitals (MOs), will be valid only if the ligand-centered orbitals from which the MOs are constructed are noninteracting.

In the present work, we extend the RCB model to treat multiply charged anions in which (a) the negatively charged sites are considerably closer together than in earlier studies and (b) there are multiple resonance structures which complicate the calculation of the internal Coulomb energy. In particular, we first examine the predictions of the RCB model when applied to MgF_4^{2-} , BeF_4^{2-} , TeF_8^{2-} , SeF_8^{2-} , and TeCl_8^{2-} for which *ab initio* data are available on the relative energies of the dianion, anion, and neutral. These systems constitute the set of species on which we test the validity and accuracy of the Coulomb model. We then apply the model to predict the energies of the states of SO_4^{2-} (relative to SO_4^{1-}), CO_3^{2-} (relative to CO_3^{1-}), and PO_4^{3-} and PO_4^{2-} (relative to PO_4^{1-} and PO_4). In the latter predictive applications, we suggest SO_4^{2-} to be metastable with respect to SO_4^{1-} by 0.75 eV, but to have a RCB of height 5.88 eV through which the departing electron must tunnel to effect autodetachment. We find CO_3^{2-} to be unstable by 1.50 eV and to have a RCB of 6.29 eV. For PO_4^{3-} , we predict the triply charged anion to lie 5.68 eV above PO_4^{2-} and to have a RCB of 10.76 eV, and PO_4^{2-} to lie 0.3 eV above PO_4^{1-} and to have a RCB or 5.38 eV.

III. *Ab Initio* and RCB Computational Methods

The equilibrium geometries of the closed-shell multiply charged anions were optimized at the MP2 level with aug-cc-pVDZ basis sets¹⁰ and final energies determined at the CCSD(T) level for the tetrahedral BeF_4^{2-} , MgF_4^{2-} , PO_4^{3-} , CO_3^{2-} , and SO_4^{2-} species. For the square antiprism structures of TeF_8^{2-} , SeF_8^{2-} , and TeCl_8^{2-} , the geometry optimization and final energy differences were performed at the SCF level, and we used the Los Alamos pseudopotential and valence double- ζ basis set (denoted LANL2DZ and implemented in the Gaussian 98 program suite¹¹) for the Te and Se atoms together with aug-cc-pVDZ basis set for the F and Cl atoms. Clearly, the modest basis sets and the level of treatment of electron correlation limit the accuracy of our calculated detachment energies. However, as we show below, the differences between the dianion–anion and anion–neutral detachment energies thereby computed display remarkable support for the simple Coulomb model. Thus, it is likely that these *differences* are more accurately reproduced than are the absolute detachment energies.

It is important to note that the trianion–dianion, dianion–anion, and anion–neutral energy differences used to calibrate the accuracy of the Coulomb model were computed at the equilibrium structures of the corresponding closed-shell dianions (or trianion in the case of PO_4^{3-}). Such frozen geometries are used because the Coulomb model itself relates to energy differences among species having the same atomic composition and nuclear positions but varying number of electrons. For this reason, the RCB model should be viewed as a means for predicting vertical electron detachment energies, not adiabatic energies.

(10) Kendall, R. A.; Dunning, T. H., Jr.; Harrison, R. J. *J. Chem. Phys.* **1992**, *96*, 6796.

(11) GAUSSIAN 98, Revision A.7, M. J. Frisch, G. W. Trucks, H. B. Schlegel, G. E. Scuseria, M. A. Robb, J. R. Cheeseman, V. G. Zakrzewski, J. A. Montgomery, Jr., R. E. Stratmann, J. C. Burant, S. Dapprich, J. M. Millam, A. D. Daniels, K. N. Kudin, M. C. Strain, O. Farkas, J. Tomasi, V. Barone, M. Cossi, R. Cammi, B. Mennucci, C. Pomelli, C. Adamo, S. Clifford, J. Ochterski, G. A. Petersson, P. Y. Ayala, Q. Cui, K. Morokuma, D. K. Malick, A. D. Rabuck, K. Raghavachari, J. B. Foresman, J. Cioslowski, J. V. Ortiz, A. G. Baboul, B. B. Stefanov, G. Liu, A. Liashenko, P. Piskorz, I. Komaromi, R. Gomperts, R. L. Martin, D. J. Fox, T. Keith, M. A. Al-Laham, C. Y. Peng, A. Nanayakkara, C. Gonzalez, M. Challacombe, P. M. W. Gill, B. Johnson, W. Chen, M. W. Wong, J. L. Andres, C. Gonzalez, M. Head-Gordon, E. S. Replogle, and J. A. Pople; Gaussian, Inc.: Pittsburgh, PA, 1998.

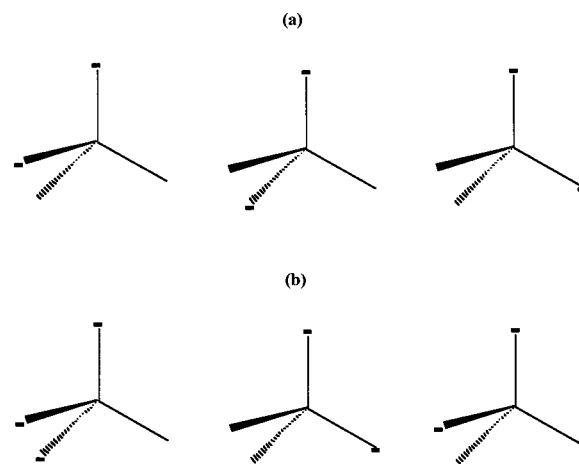


Figure 6. Resonance structures appropriate to (a) tetrahedral dianions and (b) tetrahedral trianions for removal of an electron from the top anion site.

For the dicarboxylates discussed earlier, the Coulomb energy is trivial to compute once one defines where within the $-\text{CO}_2^-$ groups the charge resides. For all of the di- and trianions treated here, the calculation is complicated by the fact that the two or three excess charges are delocalized over three or more equivalent ligand sites. The proper way to compute the Coulomb energy is to do so for each possible way of distributing the excess charges among the ligands and to then average over all such distributions. For the tetrahedral species (MgF_4^{2-} , BeF_4^{2-} , SO_4^{2-} , CO_3^{2-} , and PO_4^{3-}), the evaluation of the internal Coulomb energy is effected simply by computing e^2/R_{LL} for each resonance structure of the anion and averaging over the resonance structures. Here R_{LL} denotes the distance between any two “ligands” (i.e., the outermost atoms), which is where the excess charges are assumed to be localized. For the uncharged and singly charged species, there is zero internal Coulomb energy because there is zero or one excess charge in these cases, respectively. For the dianions and trianions, the resonance structures shown in Figure 6a,b occur with equal weight.¹² Hence, the RCB operative in the dianions is the internal Coulomb energy (averaged over the appropriate resonance states) of the dianion minus that of the anion (which is zero):

$$\text{RCB} = \frac{1}{3}(e^2/R_{LL} + e^2/R_{LL} + e^2/R_{LL}) = e^2/R_{LL} \quad (1a)$$

For the trianions, the RCB is equal to the (resonance-averaged) internal Coulomb energy of the trianion minus that of the dianion:

$$\text{RCB} = \frac{1}{3}(3e^2/R_{LL} + 3e^2/R_{LL} + 3e^2/R_{LL}) - \frac{1}{3}(e^2/R_{LL} + e^2/R_{LL} + e^2/R_{LL}) = 2e^2/R_{LL} \quad (1b)$$

However, for the square antiprism structures of TeF_8^{2-} , SeF_8^{2-} , and TeCl_8^{2-} , there is no single distance between pairs of ligands, as a result of which the resonance structures in the dianion are not all symmetry (or energy) equivalent. The seven resonance structures are shown in Figure 7, where the four distinct R_{LL} values are also defined. To compute the RCB in such cases, we assume¹³ that the seven resonance structures are equally weighted and we thus compute RCB as

$$\text{RCB} = \frac{1}{7}(e^2/R_2 + 2e^2/R_1 + 2e^2/R_3 + 2e^2/R_4) \quad (2)$$

The geometrical parameters used to compute the RCBs in the tetrahedral

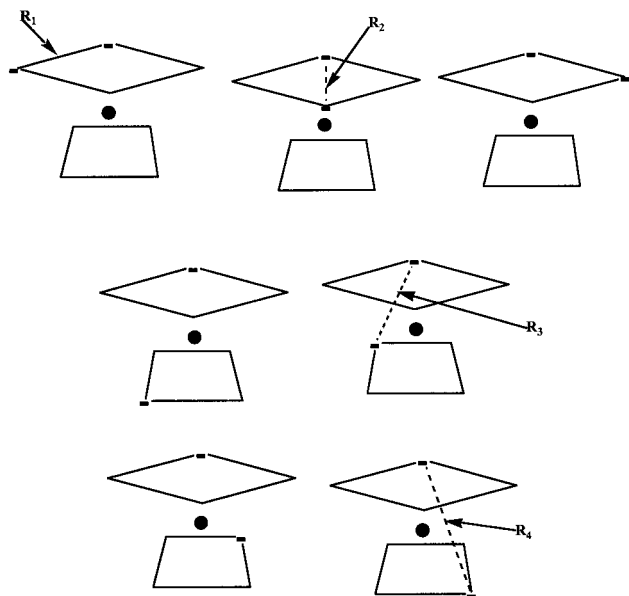
(12) In listing the resonance structures, it is sufficient to select one of the sites to represent the site from which the electron is to be detached and to then enumerate all possible locations of the other negative charge(s). One obtains the same result for the RDB if one, alternatively, also averages over all possible locations of the site from which detachment occurs.

(13) This is an assumption that we need to make to retain the simplicity of this model. Clearly, the resonance structures that have the two anion sites more distant are likely to be favored over structures with the two sites closer, so our estimate probably overestimates the RCB.

Table 1. Geometries and Coulomb and Detachment Energies of Stable Dianions

dianion	geometrical parameters (Å)	dianion Coulomb energy ^a (RCB) (eV)	dianion-to-anion detachment energy ^b (eV)	anion-to-neutral detachment energy ^{b,c} (eV)	difference in detachment energies (eV)
BeF ₄ ²⁻	$R_{FF} = 2.66$	5.41	1.68	7.03	5.35
MgF ₄ ²⁻	$R_{FF} = 3.17$	4.54	2.65	7.21	4.56
TeF ₈ ²⁻	$R_1 = 2.26, R_2 = 3.20, R_3 = 2.40, R_4 = 3.61$	5.31	4.91	9.98	5.07
SeF ₆ ³⁻	$R_1 = 2.19, R_2 = 3.10, R_3 = 2.33, R_4 = 3.50$	5.48	5.7 ^d	11.2 ^d	5.5
TeCl ₈ ²⁻	$R_1 = 3.09, R_2 = 4.38, R_3 = 3.28, R_4 = 4.94$	3.88	4.3 ^d	8.0 ^d	3.7

^a Coulomb energies computed as in eqs 1 and 2. ^b Detachment energies computed at the equilibrium geometry of the dianion. ^c These energies reflect the intrinsic electron binding strengths in the absence of any Coulomb repulsion. ^d Reported only to this precision in ref 2k.

**Figure 7.** Resonance structures appropriate to square antiprism dianions.

and square antiprism species considered here are given in Table 1 along with the resultant RCB values.

Before examining the results obtained with the Coulomb model for these test systems, we should again mention that it is not obvious that the model will work when applied to such species because it is not clear that the orbitals from which electrons are removed are sufficiently localized and noninteracting. Finally, when computing the second electron detachment energy (e.g., the SO_4^- to SO_4 energy in the case of the SO_4^{2-} dianion), we use the energy of the triplet state to most correctly represent the lowest state for a species with electrons removed from two different orbitals.

IV. Results of Applying the RCB Model

A. Tests on Electronically Stable Dianions. Shown in Table 1 are the ab initio computed dianion–anion–neutral energy differences for the dianions used here as cases on which to test the validity of the RCB model. It should again be noted that all of the electron detachment energies (EDEs) are energies computed at the equilibrium geometry of the dianion. By keeping the geometry frozen in our calculations, we are able to isolate the contributions to the EDE made by the internal Coulomb repulsion and by the intrinsic attractive valence-orbital potentials.

For the test cases considered here, if the Coulomb model were entirely correct, the differences between the EDEs of the dianion and the anion should equal the internal Coulomb energy of the dianion. That is, the energies displayed in the third and sixth columns of Table 1 would agree if the model were accurate. Our ability to relate the first and second electron detachment energies to the RCB, of course, also depends on the extent to

which the orbitals from which the two electrons are removed are spatially separated and nonoverlapping. For MgF_4^{2-} , the t_1 , t_2 , and e molecular orbitals comprised of fluorine 2p basis orbitals have SCF orbital energies of -0.162 , -0.173 , and -0.178 H, respectively. For SO_4^{2-} , these same orbital energies are -0.33 , -0.35 , and -0.55 H.

As the data of Table 1 clearly show, the model works quite well, and the largest discrepancy between its prediction and the ab initio calculated differences in EDEs, which occurs for TeF_8^{2-} , is 0.24 eV. The average deviation in the ab initio and model energy differences is 0.10 eV for the five test cases. Because the model calculates the RCB in terms of the distances between atomic centers rather than between orbital centroids, it likely overestimates the RCB values. However, the data of Table 1 show that this overestimate is not severe for the test anions considered here.

B. Predictions for Metastable Multiply Charged Anions.

The SO_4^{2-} , CO_3^{2-} , and PO_4^{3-} ions are known to be unstable with respect to electron loss in the gas phase.¹⁴ However, it is probable that these species, as in the $\text{CuPc}(\text{SO}_3)_4$ case discussed earlier, have metastable ground states in which an electron must tunnel through a RCB to escape. With this possibility in mind, we make use of the Coulomb model to predict (a) the RCBs, (b) the energies of the $(-n)$ charged anions relative to the $(-n + 1)$ charged anions, and (c) the tunneling lifetimes of the $(-n)$ charged anions for the species listed.

In the tetrahedral SO_4^{2-} case, the internal Coulomb energy of the dianion computed as in eq 1a is $e^2/R_{00} = 5.88$ eV (see Table 2 where the requisite geometry and energy data are given). Of course, the Coulomb energy of the singly charged anion SO_4^- is zero, so the RCB for detachment of an electron from SO_4^{2-} is equal to 5.88 eV. For PO_4^{3-} and PO_4^{2-} , there are two distinct internal Coulomb energies that must be computed. For the doubly charged PO_4^{2-} , the internal Coulomb energy again is given as in eq 1a ($e^2/R_{00} = 5.38$ eV). This is the RCB to use in the PO_4^{2-} to PO_4^{1-} detachment. In the PO_4^{3-} case, the total internal Coulomb energy averaged over the three resonance structures in Figure 6b is $1/3(3e^2/R_{00} + 3e^2/R_{00} + 3e^2/R_{00}) = 3e^2/R_{00}$. For detaching an electron from PO_4^{3-} to form PO_4^{2-} , the RCB is as given in eq 1b, $2e^2/R_{00} = 10.76$ eV.

To obtain further testing of the RCBs computed above, we also carried out a series of ab initio calculations on SO_4^{1-} with a negative “test charge” placed at various distances r and different orientations to generate, as done in ref 9a, a potential energy surface appropriate for an attaching electron.¹⁵ We found a surface whose Coulomb barrier is obtained as the test charge approaches along one of the S–O bond axes. The height of the Coulomb barrier thus obtained was 4.37 eV. As noted above, the RCB model tends to overestimate Coulomb barriers because it computes them in terms of internuclear distances rather than orbital centroid distances. It may be for this reason that the

(14) See, for example: Boldyrev, A. I.; Simons, J. J. *Phys. Chem.* **1994**, *98*, 2293.

Table 2. Dianion and Trianion Energies from the Coulomb Model for Metastable Anions

detachment event	geometrical parameters (Å)	repulsive Coulomb barrier ^a (RCB) (eV)	trianion-to-dianion detachment energy (eV)	dianion-to-anion detachment energy (eV)	anion-to-neutral detachment energy ^b (BE) (eV)
SO ₄ ²⁻ → SO ₄ ¹⁻	R _{OO} = 2.45	5.88		-0.75 ^a	5.13
CO ₃ ²⁻ → CO ₃ ¹⁻	R _{OO} = 2.29	6.29		-1.50 ^a	4.79
PO ₄ ²⁻ → PO ₄ ¹⁻	R _{OO} = 2.67	5.38		-0.30 ^a	5.08
PO ₄ ³⁻ → PO ₄ ²⁻		10.76	-5.68 ^a		

^a Predicted using the Coulomb model. ^b Ab initio calculated at the equilibrium geometry of the $(-n)$ charged anion. These energies reflect the intrinsic electron binding strengths in the absence of any Coulomb repulsion.

barrier obtained by the test charge method is somewhat smaller than the RCB value (5.88 eV) obtained above using the Coulomb model. However, as shown later, the lifetimes we obtain within our Coulomb model or using this test charge potential vary by less than an order of magnitude. This comparison, together with that presented below for PtCl₄²⁻ and the comparisons with ab initio data given earlier for the test systems MgF₄²⁻, BeF₄²⁻, TeF₈²⁻, SeF₈²⁻, and TeCl₈²⁻ offer significant reasons to trust this easy-to-use model. We, therefore, move on to consider the energies and lifetimes of the metastable species mentioned above.

The energies of SO₄²⁻, CO₃²⁻, PO₄³⁻, and PO₄²⁻ relative to SO₄¹⁻, CO₃¹⁻, PO₄²⁻, and PO₄¹⁻, respectively, can be predicted by (1) using the ab initio calculated (at the dianion geometry) SO₄ → SO₄¹⁻, CO₃ → CO₃¹⁻, and PO₄ → PO₄¹⁻ energy differences, which reflect the intrinsic binding energies (BE) of the valence potentials absent any Coulomb repulsion and (2) shifting this energy upward by the appropriate RCB to reflect the destabilizing effect of the Coulomb repulsion between the ejected electron and the daughter anion.

For example, the PO₄²⁻ → PO₄¹⁻ energy difference is computed by taking -5.08 eV (the energy of the electron in PO₄¹⁻) and adding + 5.38 eV (the RCB of PO₄²⁻), so PO₄²⁻ is predicted to be 0.30 eV *unstable* with respect to PO₄¹⁻ plus a free electron. In Table 2 we summarize this prediction as well as those obtained using this same process on the PO₄³⁻ → PO₄²⁻ and SO₄²⁻ → SO₄¹⁻ cases.

Applying this process to the species listed, the Coulomb model suggests that (1) SO₄²⁻ is unstable by 0.75 eV with respect to electron loss, but tunneling through a barrier lying 5.88 - 0.75 = 5.13 eV above this state is necessary for electron detachment, (2) CO₃²⁻ is unstable by 1.50 eV with respect to electron loss, but tunneling through a barrier lying 6.29 - 1.50 = 4.79 eV above this state is required, (3) PO₄³⁻ is unstable by 5.68 eV with respect to electron loss, but tunneling through a barrier of 10.76 - 5.68 = 5.08 eV is necessary, and (4) PO₄²⁻ is further unstable by 0.30 eV with respect to electron loss, but tunneling through a barrier of 5.38 - 0.30 = 5.08 eV is necessary for it to detach an electron.

B. Tunneling Lifetimes. By using a simple radial potential such as that shown in Figure 8, we have computed the tunneling probability and the tunneling rates for the SO₄²⁻, CO₃²⁻, PO₄³⁻, and PO₄²⁻ metastable species whose energies were discussed earlier. For each of these calculations, the RCB and R_{LL} values are given in Table 2, and the resultant lifetimes¹⁶ are given in

(15) It should be stressed that by no means is such an energy surface a fully rigorous concept. In computing such surfaces, (a) one must sample directions for the test charge approaching the anion that allow the test charge to reach the region (i.e., the orbital) where the "extra" electron resides in the dianion and (b) one is treating the "extra" electron as distinguishable from the other electrons. In a sense, one generates a Born-Oppenheimer (BO) like energy surface upon which the "extra" electron moves. However, because the extra electron (a) is indistinguishable from the other electrons and (b) by no means moves slowly compared to the other electrons, such a BO-like approximation is likely to be not very accurate.

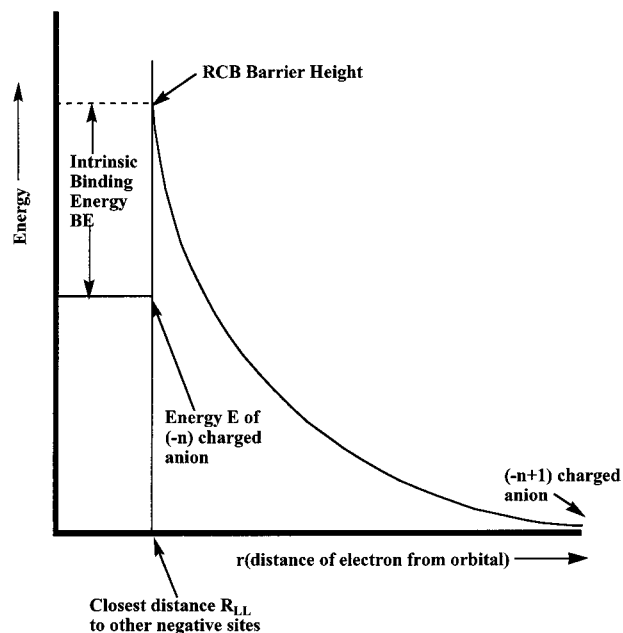
**Figure 8.** Model radial potential used to compute tunneling lifetimes in terms of repulsive Coulomb barrier height, closest distance between electrons (R_{LL}), and electron energy.

Table 3. It should be noted that the PO₄²⁻ lifetime is of no experimental relevance because it is computed at the geometry of the PO₄³⁻ trianion. The data on PO₄³⁻, CO₃²⁻, and SO₄²⁻ suggest that PO₄³⁻ is so short-lived as to render its experimental detection very difficult but that CO₃²⁻ and SO₄²⁻ should be long enough lived to be subject to experimental study.

As a final test of the Coulomb model's ability to predict tunneling lifetimes of such metastable dianions, we applied it to the PtCl₄²⁻ species that was very recently examined by other means.^{9a,1q} In the earlier work, the effective potential energy experienced by a negative "test charge" in the presence of a PtCl₄¹⁻ anion was computed as the test charge approached (a) along a Pt-Cl bond axis, (b) between two Pt-Cl bond axes, and (c) along the C₄ axis of this planar anion. The energies along these three approach directions displayed long-range Coulomb repulsion, a barrier at intermediate distances, and short-range valence attraction. Using the path with the lowest such barrier (ca. 3.3-3.5 eV) and employing an energy^{9a,1q} for the dianion of 0.23 eV above that of PtCl₄¹⁻, a lifetime of ca. 2.5 s was obtained when the requisite tunneling integral was evaluated.^{9a} To compare the predictions of the Coulomb model with these results, we first carried out ab initio calculations to

(16) The lifetime is computed as $\tau = (2R_{LL}/(2E))^{1/2} \exp\{2\int_{R_{LL}}^{Q/E} (2Q/r - E)^{1/2} dr\}$, where the integral ranges from $r = R_{LL} = Q/RCB$ to $r = Q/E$, the outer turning point for tunneling. Here $Q = 1$ for dianion detachment, and $Q = 2$ for trianion detachment. The energy of the $(-n)$ charged anion E as well as R_{LL} must be used in atomic units (i.e., hartrees and bohrs, respectively). An order-of-magnitude estimate for τ can be obtained by approximating the tunneling integral by a single term: $\tau \approx (2R_{LL}/(2E))^{1/2} \exp\{(2(RCB - E))^{1/2}(Q/E - Q/RCB)\}$.

Table 3. Predicted Dianion and Trianion Lifetimes Based on Coulomb Model

detachment event	repulsive Coulomb barrier (eV)	trianion-to-dianion detachment energy (eV)	dianion-to-anion detachment energy (eV)	tunneling lifetime (s)
$\text{SO}_4^{2-} \rightarrow \text{SO}_4^{1-}$	5.88		-0.75	$2.7 \times 10^{-8}{}^b$
$\text{CO}_3^{2-} \rightarrow \text{CO}_3^{1-}$	6.29		-1.50	1.3×10^{-11}
$\text{PO}_4^{2-} \rightarrow \text{PO}_4^{1-}$	5.38		-0.30 ^a	1.3×10^{-1}
$\text{PO}_4^{3-} \rightarrow \text{PO}_4^{2-}$	10.76	-5.68		9.4×10^{-14}

^a The PO_4^{2-} lifetime is computed at the geometry of PO_4^{3-} and, thus, is of no direct experimental relevance. ^b See ref 18.

optimize the square-planar geometry of PtCl_4^{21} and obtained $R_{\text{Cl,Cl}} = 3.37 \text{ \AA}$ (at the MP2/SBKJ+3(sp)1d on Cl and 4(sp)3d on Pt level); this geometry is close to that used in ref 9a. We thus were able to compute the internal Coulomb energy of PtCl_4^{2-} to be 3.86 eV.¹⁷ Using the energy $E = 0.23 \text{ eV}$ cited in ref 9a and our $\text{RCB} = 3.86 \text{ eV}$ in the Coulomb model potential shown in Figure 8, we computed a lifetime of 8.9 s, in reasonable agreement with the 2.5 s value obtained using the test charge potential method^{9a} discussed above.

(17) We assume that the three resonance structures, two having the two negative charges adjacent and the other with the two charges opposite one another, are equally weighted. In this manner we compute $\text{RCB} = 3.86 \text{ eV}$.

(18) We also estimated this lifetime using the test charge method employed in ref 9a by first computing the potential energy of a point negative charge interacting with a SO_4^{1-} anion. As the point charge is moved inward (from 15 Å) along one of the S–O internuclear axes, we found a potential having a barrier of height 4.4 eV, which is smaller than the 5.88 eV estimate of the Coulomb model. Using $\text{RCB} = 4.4 \text{ eV}$ and $R_{\text{LL}} = 3.3 \text{ \AA}$ (the value obtained from the maximum in our computed test charge potential calculation), we predict a lifetime of $6.0 \times 10^{-9} \text{ s}$, assuming that the resonance state has $E = 0.75 \text{ eV}$. Not surprisingly, the smaller barrier obtained in the test charge method yields a shorter lifetime than that ($2.7 \times 10^{-8} \text{ s}$) obtained with the Coulomb model's RCB . These findings are offered to suggest how the predicted lifetimes vary with changes in the RCB and R_{LL} parameters.

V. Summary

A simple model based on evaluating the Coulomb repulsion energies among negatively charged sites within spatially compact dianions and trianions has been utilized to predict trianion-to-dianion and dianion-to-anion detachment energies given the anion-to-neutral detachment energy (at the same geometry). These predictions have been shown to be reliably accurate, compared to ab initio calculated data, on the test cases examined (MgF_4^{2-} , BeF_4^{2-} , TeF_8^{2-} , SeF_8^{2-} , and TeCl_8^{2-}). This same model was then extended to make predictions of the energies of resonance states of metastable dianions (SO_4^{2-} , CO_3^{2-} , and PO_4^{2-}) as well as the PO_4^{3-} trianion, as well as to estimate the tunneling lifetimes of these metastable states. The model is expected to be applicable when the orbitals from which the two electrons are removed are nearly isoenergetic and nonoverlapping (e.g., as in MgF_4^{2-} where the t_1 , t_2 , and e nonbonding orbitals range from -0.163 to -0.178 H).

Acknowledgment. This work was supported by NSF Grants CHE9618904 and CHE9982420. The computer time provided by the Center for High Performance Computing at the University of Utah is also gratefully acknowledged.

JA001936A